HHS Public Access

Author manuscript

Nucl Med Biol. Author manuscript; available in PMC 2020 January 14.

Published in final edited form as:

Nucl Med Biol. 2013 January ; 40(1): 141–147. doi:10.1016/j.nucmedbio.2012.08.011.

Synthesis and biological evaluation of [^{11}C]SB366791: A new PET-radioligand for *in vivo* imaging of the TRPV1 receptor

Daisy van Veghel[a], **Jan Cleynhens**[a], **Larry V. Pearce**[b], **Peter M. Blumberg**[b], **Koen Van Laere**[c], **Alfons Verbruggen**[a], **Guy Bormans**[a,*]

[a]Laboratory for Radiopharmacy, KU Leuven, Leuven, Belgium

[b]Laboratory of Cancer Biology and Genetics, Center for Cancer Research, National Cancer Institute, National Institutes of Health, Bethesda, MD 20892-4255, USA

[c]Division of Nuclear Medicine, University Hospital and KU Leuven, Leuven, Belgium

Abstract

Introduction: The transient receptor potential vanilloid subfamily member 1 (TRPV1) receptor, a non-selective cation channel, is known for its key role in pain nociception and neurogenic inflammation. TRPV1 expression has been demonstrated in diverse tissues and an essential role for TRPV1 in various disorders has been suggested. A TRPV1-specific PET-radioligand can serve as a useful tool for further *in vivo* research in animals and directly in humans. In this study, we report the synthesis and biological evaluation of a carbon-11 labelled analogue of N-(3-methoxyphenyl)-4-chlorocinnamide (SB366791) which was reported as a specific high-affinity antagonist for TRPV1.

Methods: The new tracer was evaluated with respect to log D and biodistribution in control, pretreated and TRPV1$^{-/-}$ mice. The percentage of radiometabolites of [^{11}C]SB366791 was determined in mouse plasma and brain.

Results: [^{11}C] SB366791 was obtained in good yield (69%±11%; isolated amounts 3034–5032 MBq) and high specific activity (390±215 GBq/μmol). The tracer was efficiently cleared from blood and all major organs via hepatobiliary and renal pathways. Initial brain uptake was high (1.6% ID) and wash-out from brain was rapid. The retention of [^{11}C] SB366791 in the trigeminal nerve of control mice was prominent. The *in vitro* binding affinity of SB366791 was determined to be 280±56 nM and 780±140 nM for human and rat TRPV1, respectively.

Conclusions: [^{11}C] SB366791 has favourable biodistribution characteristics in mice. However the obtained low binding affinity for TRPV1 may not be sufficient to use the current compound as PET tracer.

Keywords

TRPV1; Positron emission tomography [^{11}C]SB366791

*Corresponding author. Laboratory for Radiopharmacy, Campus Gasthuisberg O&N2, Herestraat 49 Box 821, BE-3000 Leuven, Belgium. Tel.: +32 16 330447; fax: +32 16 330449.

1. Introduction

In 1997 the transient receptor potential vanilloid subfamily member 1 (TRPV1) receptor was cloned by David Julius and colleagues as a functional capsaicin-sensitive receptor [1]. Since its discovery, an immense interest in TRPV1 has arisen. TRPV1 is a non-selective, Ca^{2+} permeable cation channel belonging to the extended family of TRP ion channels. Each TRPV1 protein comprises six transmembrane regions (TM1-TM6), a short pore-forming region between TM5 and TM6 and cytosolic N- and C-termini [2]. The functional channel is a tetrameric membrane protein consisting of four identical TRPV1 subunits with a central pore and it can be activated by various noxious stimuli such as exogenous (capsaicin, resiniferatoxin (RTX)) or endogenous (anandamide) agonists, heat and acidic pH [3,4]. So far, the ligand-binding sites of TRPV1 are not fully identified. The residues Y511 and S512 located between TM2 and TM3 in the cytosolic region of TRPV1 are crucial for binding of capsaicin to TRPV1, whereas L547 (human) or M547 (rat) is necessary for TRPV1-RTX interaction. Further structural elements may also contribute to TRPV1 activation [5]. TRPV1 is mainly expressed on small-diameter neurons with non-myelinated C-fibers, and on a subset of myelinated Aδ-neurons of the dorsal root and trigeminal ganglia. These primary sensory neurons integrate nociceptive information from the periphery into the central nervous system and play an essential role in the generation and progression of neurogenic inflammation after tissue injury or in chronic inflammatory conditions. Activation of TRPV1 expressing neurons results in the release of pro-inflammatory neuropeptides such as substance P and calcitonin-gene-related peptide (CGRP) that, in turn, trigger inflammatory cascades, oedema and pain [4,6–8]. Moreover, it has been suggested that TRPV1 is involved in the pathogenesis of various pain conditions such as nerve damage induced hyperalgesia, diabetic neuropathy and cancer pain [9]. Therefore, TRPV1 has become a promising pharmacological target for the development of new anti-inflammatory and analgesic drugs. Qutenza®, a high-concentration capsaicin dermal patch, has recently been approved in both the EU and USA for the treatment of peripheral neuropathic pain [10]. Clinical trials are ongoing to evaluate the therapeutic potential of various TRPV1 agonists and antagonists for the treatment of chronic inflammatory disorders such as osteoarthritis and migraine and for the treatment of various pain conditions [11].

As in nociceptive neurons, functional expression of TRPV1 has also been identified in various non-neuronal cell types, including diverse human skin cells [12], urothelial cells [13] and pancreatic β-cells [14]. Recent data suggest that TRPV1 receptors expressed in urothelial cells are involved in the micturition reflex and cystitis [13] and that TRPV1 in pancreatic β-cells modulates insulin secretion [14]. Nevertheless, the exact (patho)physiological role of TRPV1 in non-neuronal cells remains elusive.

Accumulating evidence indicates the existence of a functionally active population of TRPV1 receptors in brain tissue, but the extent to which TRPV1 channels are expressed in the central nervous system (CNS) remains a subject of controversy [6,15–18]. Co-expression of TRPV1 with type 1 cannabinoid (CB1) receptors in various brain regions such as the hippocampus [19], the presence of potent, TRPV1-activating endovanilloids (e.g. anandamide) in several brain regions [20], and the different behavioural responses that have been observed between $TRPV1^{-/-}$ mice and wild-type mice [20,21] strongly suggest a

functional role for TRPV1 receptors in the CNS. Hypothalamic TRPV1 receptors play a role in thermoregulation [9] and TRPV1 activation elicits a form of long-term depression (LTD) in hippocampal neurons, which was absent in TRPV1$^{-/-}$ mice, suggesting that TRPV1 channels may play a key role in learning, the control of emotions and epileptic activity [22]. Furthermore, evidence raises that TRPV1 channels contribute to the pathogenesis of febrile seizures, stroke and neurodegenerative brain disorders such as Parkinson's disease [20,23].

A PET-radioligand that specifically binds TRPV1 with high affinity may serve as a powerful tool for further *in vivo* research to investigate TRPV1 expression under (patho)physiological conditions, and to study the pharmacodynamic properties of therapeutics that target TRPV1. To our knowledge, no TRPV1-specific PET-radioligand has been developed so far. In this study, we have synthesized a carbon-11 labelled analogue of *N*-(3-methoxyphenyl)-4-chlorocinnamide (SB366791), a potent (IC_{50} reported for hTRPV1=5.7 nM) and selective TRPV1 antagonist developed by GSK [24], and evaluated its potential to visualize TRPV1 *in vivo*.

2. Materials and methods

2.1. Chemicals and general instrumentation

4-Chlorocinnamic acid was obtained commercially from Sigma-Aldrich (Bornem, Belgium). All other reagents and solvents were purchased from Acros Organics (Geel, Belgium) or Fisher Scientific (Erembodegem, Belgium) and were used without further purification. Capsaicin was obtained from Calbiochem (now EMD Chemicals, San Diego, CA, USA). Resiniferatoxin (RTX) was purchased from LC Laboratories (Woburn, MA, USA). [^{3}H]RTX (1 GBq/mmol) was obtained from Perkin Elmer (Boston, MA, USA) through a licensing agreement. Dulbecco's Modified Eagle Medium (DMEM, 1×), Dulbecco's Phosphate Buffered Saline (DPBS, 1×), Ham's F-12 medium and Geneticin were purchased from Invitrogen (Grand Island, NY, USA). Tetracycline was purchased from EMD Chemicals (San Diego, CA, USA). Foetal bovine serum was obtained from Gemini Bio-Products (West Sacramento, CA, USA) and bovine serum albumin (Cohn fraction V) was obtained from Sigma-Aldrich (St. Louis, MO, USA). Bovine glycoprotein (fraction VI) and [^{45}Ca]$CaCl_2$ were purchased from MP Biomedicals (Solon, OH, USA).

For ascending thin layer chromatography (TLC), pre-coated aluminium backed plates (Silica gel 60 with fluorescent indicator UV 254 nm, 0.2 mm thickness; Macherey-Nagel, Düren, Germany) were used and developed using mixtures of ethyl acetate (EtOAc) and heptane as mobile phase. After evaporation of the solvent, compounds were detected under UV light (254 nm). Column chromatography was performed using silica gel (silica 60–200, 60 Å, Acros, Geel, Belgium). ^{1}H nuclear magnetic resonance (NMR) spectra were acquired with a Bruker Avance II spectrometer (400 MHz, 5 mm probe, Fällanden, Switzerland) using deuterated methanol (MeOD) or deuterated dimethyl sulfoxide (DMSO-d_6) as solvent. Chemical shifts are reported in parts per million relative to tetramethylsilane ($\delta = 0$). Coupling constants are reported in hertz (Hz). Splitting patterns are defined by s (singlet), d (doublet) or t (triplet). High-performance liquid chromatography (HPLC) analysis was performed on a Merck Hitachi L2130 LaChrom Elite pump (Hitachi, Tokyo, Japan) connected to a UV L2400 LaChrom Elite spectrometer (Hitachi). Radioactivity in the HPLC

effluent was monitored by a 3-in. NaI(Tl) scintillation detector connected to a single channel analyzer (GABI box; Raytest, Straubenhardt, Germany). Data were acquired and analyzed using the RaChel (Lablogic, Sheffield, UK) or GINA Star (Raytest) data acquisition system. Quantification of radioactivity during biodistribution and metabolite studies was performed using an automated gamma counter equipped with a 3-in. NaI(Tl) well crystal coupled to a multichannel analyzer, mounted in a sample changer (Wallac 1480 Wizard 3q, Wallac, Turku, Finland). The values are corrected for background radiation, physical decay and counter dead time.

All animal experiments were performed in compliance with the principles set by the Belgian law relating to the conduct of animal experimentation, after approval from the university animal ethics committee. Animals were housed in individually ventilated cages in a thermo-regulated (22 °C), humidity-controlled facility under a 12 h light/12 h dark cycle, with free access to food and water. TRPV1$^{-/-}$ mice were kindly provided by Professor T. Voets (Laboratory of Ion Channel Research, KU Leuven, Belgium).

2.2. Synthesis of N-(3-hydroxyphenyl)-4-chlorocinnamide (4) and N-(3-methoxyphenyl)-4-chlorocinnamide (SB366791)

2.2.1. 2-(3-Acetamidophenoxy)tetrahydro-2 H-pyran (1)—To a solution of 3-acetamidophenol (6 g, 39.6 mmol) in CH_2Cl_2 (50 mL) was added pyridinium *p*-toluenesulfonate (PPTS; 200 mg, 0.79 mmol) and 3,4-dihydro-2 H-pyran (6.4 mL). The reaction mixture was stirred at ambient temperature under N_2 for 16 h and washed with 1 M NaOH. After drying over $MgSO_4$, the filtrate was concentrated in vacuo to obtain **1** as a solid white powder, which was used in the next step without further purification.

2.2.2. 2-(3-Aminophenoxy)tetrahydro-2 H-pyran (2)—A mixture of **1** (2.35 g, 10 mmol), NaOH (1 g, 25 mmol), water (1.5 mL) and ethylene glycol (4 mL) was stirred for 4 h at 130 °C. After cooling to room temperature, the solution was diluted with water (5 mL) and extracted with CH_2Cl_2. The organic layer was washed with 0.1 M NaOH, dried over $MgSO_4$ and filtered. The solvent was removed under reduced pressure to obtain a brownish oil **2** (1.31 g, 6.78 mmol), which was used as such in the next step.

2.2.3. 2-[3-(4-Chlorocinnamido)phenoxy]tetrahydro-2 H-pyran (3)—1-(3-Dimethylaminopropyl)-3-ethylcarbodiimide hydrochloride (EDCI; 0.99 g, 5.17 mmol) and 1-hydroxybenzotriazole hydrate (HOBt; 0.70 g, 5.17 mmol) were added to a solution of 4-chlorocin-namic acid (0.86 g, 4.60 mmol) in DMF (30 mL). After stirring for 20 min at room temperature, **2** (1.00 g, 5.17 mmol) was added to the reaction mixture and stirring was continued for 16 h at room temperature. The reaction mixture was concentrated under reduced pressure. The residue was dissolved in EtOAc, washed with 1 M HC1 and water, dried with $MgSO_4$ and again concentrated under reduced pressure. The residue was purified by silica gel column chromatography eluted with a mixture of heptane and EtOAc (3:1 V/V). The solvent was removed under reduced pressure and the final product (357 mg, 1 mmol) was crystallized from ether. Yield (relative to 3-acetamidophenol): 5.7%. TLC (EtOAc/heptane 1:1): R_f =0.7. MS (ES)$^+$: m/z $[C_{20}H_{20}ClNO_3 + H]^+$: theoretical 358 Da, measured 358 Da.

^{1}H NMR (DMSO-d_6,) δ 7.65 (2H, d, $^3J_{H-H}$=8.5Hz, H_{3Ar-Cl} and H_{5Ar-Cl}); 7.51 (2 H, d, $^3J_{H-H}$ =8.5 Hz, H_{2Ar-Cl} and H_{6Ar-Cl}); 7.57 (1 H, d, $^3J_{H-H}$ = 15.7 Hz, -*CH*CHCO-); 6.83 (1 H, d, $^3J_{H-H}$=15.7 Hz, -CH*CHCO*-); 10.20 (1 H, s, -CO*NH*-); 7.20–7.31 (3 H, m, H_{4Ar-O}, H_{5Ar-O} and H_{6Ar-O}); 7.49 (1 H, s, H_{2Ar-O}); 6.73–6.77 (1 H, m, H_{1THP}); 3.75–3.81 (1 H, m, H_{3aTHP}); 3.53–3.59 (1 H, m, H_{3bTHP}); 1.71–1.89 (3 H, m, H_{4THP} and H_{6aTHP}); 1.53–1.65 (3 H, m, H_{5THP} and H_{6bTHP}).

2.2.4. N-(3-hydroxyphenyl)-4-chlorocinnamide (4)—A mixture of **3** (357 mg, 1 mmol), PPTS (12 mg) and ethanol (EtOH; 10 mL) was stirred for 18 h at 45 °C. After addition of toluene (10 mL) and triethylamine (NEt_3; 1 mL), the mixture was concentrated under reduced pressure and the residue was dissolved in EtOAc (15 mL). The organic layer was washed with brine, dried over $MgSO_4$ and concentrated to afford product **4** (143 mg, 0.52 mmol). Yield: 52%. TLC (EtOAc/heptane 1:1): R_f =0.4. HPLC (CH_3CN/ammonium acetate (NH_4OAc) 0.05 M pH=5.5 65:35 V/V; 1 mL/min): t_R =5.2 min (99%). LC-MS (ES)$^+$: m/z $[C_{15}H_{12}ClNO_2$ +H$]^+$: theoretical 274 Da, measured 274 Da.

^{1}H NMR (DMSO-d_6,) δ 7.64 (2H, d, $^3J_{H-H}$=8.3Hz, H_{3Ar-Cl} and H_{5Ar-Cl}); 7.50 (2H, d, $^3J_{H-H}$=8.3 Hz, H_{2Ar-Cl} and H_{6Ar-Cl}); 7.55 (1H, d, $^3J_{H-H}$= 15.7 Hz, -*CH*CHCO-); 6.82 (1H, d, $^3J_{H-H}$=15.7Hz, -CH*CHCO*-); 10.09 (1H, s, -CO*NH*-); 7.04 (1H, d, $^3J_{H-H}$=7.7Hz, H_{6Ar-OH}); 7.10 (1H, t, $^3J_{H-H}$= 7.7 Hz, H_{5Ar-OH}); 6.47 (1 H, d, $^3J_{H-H}$=7.7 Hz, H_{4Ar-OH}); 7.29 (1 H, s, H_{2Ar-OH}); 9.44 (1 H, s, Ar-*OH*).

2.2.5. 4-Chlorocinnamoyl chloride (5)—A mixture of commercially available 4-chlorocinnamic acid (2.74 g, 15 mmol) and thionyl chloride ($SOCl_2$; 10 mL, 138 mmol) was refluxed under stirring for 2 h. The reaction mixture was allowed to cool to room temperature and the residual $SOCl_2$ was removed under reduced pressure to obtain compound **5**. The crude product **5** was used as such in the next step, without further purification.

2.2.6. N-(3-methoxyphenyl)-4-chlorocinnamide (SB366791)—A solution of 3-methoxyaniline (12.5 mmol) in a mixture of toluene (70 mL) and NEt_3 (12.5 mmol) was added drop-wise to an ice-cold solution of **5** (3.0 g, 14.9 mmol) in toluene (50 mL). The reaction mixture was allowed to warm to room temperature and was stirred for 2 h. The precipitate was collected by filtration, washed successively with an aqueous solution of 5% sodium bicarbonate (100 mL) and water (100 mL) and dried overnight in an oven under reduced pressure. The dried precipitate was recrystallized from EtOH. Yield (relative to 4-chlorocinnamic acid): 55%. TLC (EtOAc/heptane 1:1): R_f =0.6. HPLC (CH_3CN/NH_4OAc 0.05 M pH=5.5 65:35 V/V; 1 mL/ min): t_R =8.2 min (N99%). LC-MS (ES)$^+$: m/z $[C_{16}H_{14}ClNO_2$ +H$]^+$: theoretical 288 Da, measured 288 Da.

^{1}H NMR (DMSO-d_6) δ 7.65 (2H, d, $^3J_{H-H}$=8.3 Hz, H_{3Ar-Cl} and H_{5Ar-Cl}); 7.50 (2H, d, $^3J_{H-H}$=8.3 Hz, H_{2Ar-Cl} and H_{6Ar-Cl}); 7.57 (1H, d, $^3J_{H-H}$= 15.7Hz, -*CH*CHCO-); 6.82 (1H, d, $^3J_{H-H}$=15.7Hz, -CH*CHCO*-); 10.22 (1H, s, -CO*NH*-); 7.21 (1H, d, $^3J_{H-H}$=7.7Hz, $H_{6Ar-OCH3}$); 7.24 (1H, t, $^3J_{H-H}$= 7.7 Hz, $H_{5Ar-OCH3}$); 6.66 (1 H, d, $^3J_{H-H}$=7.7 Hz, $H_{4Ar-OCH3}$); 7.41 (1 H, s, $H_{2Ar-OCH3}$); 3.74 (1 H, s, Ar-O*CH$_3$*).

2.3. Radiosynthesis

Carbon-11 was obtained in the form of [^{11}C]CH_4 by a ^{14}N(p,α)^{11}C nuclear reaction in a Cyclone 18/9 cyclotron (IBA Louvain-la-Neuve, Belgium). [^{11}C]CH_4 was converted to [^{11}C]CH_3I in a home-built gas phase recirculation module. [^{11}C]CH_3I was bubbled with a flow of helium through a solution of **4** (200 μg) in DMF (200 μL) in the presence of cesium carbonate (Cs_2CO_3, 2–3 mg). When the amount of radioactivity in the reaction vial was stabilized, the reaction mixture was heated for 5 min at 70 °C. The crude reaction mixture was diluted with a mixture of 30% EtOH in 0.05 M NH_4OAc pH 5.5 (1.8 mL) and applied on an HPLC column (XTerra RP18, 5 μm, 7.8 mm×150 mm; Waters) eluted with a mixture of 0.05 M NH_4OAc (pH 5.5) and EtOH (35:65 V/V) at a flow rate of 1.5 mL/min. UV detection of the HPLC eluate was performed at 254 nm. The radiolabelled product [^{11}C] SB366791 was collected after 10 min. Quality control was performed on an analytical HPLC system consisting of a column (XTerra RP18, 5 μm, 4.6×250 mm; Waters) eluted with a mixture of CH_3CN and NH_4OAc buffer 0.05 M pH 5.5 (65:35 V/V) at a flow rate of 1 mL/min. UV detection was performed at 263 nm.

2.4. Distribution coefficient

HPLC-purified [^{11}C]SB366791 was diluted in saline to obtain a concentration of~37 MBq/mL. A 25 μL aliquot of this solution was added to a plastic tube containing 0.025 M sodium phosphate buffer pH 7.4 (2 mL, density=1.000 g/mL) and n-octanol (2 mL, density= 0.827 g/mL) (n=8). The tube was vortexed at room temperature for 1 min and then centrifuged at 3000 rpm for 10 min. Aliquots of 50 μL and 500 μL were taken from the *n*-octanol phase and aqueous phase, respectively, and transferred into separate tared vials. Cross contamination between the two phases was avoided. The samples were weighed and their radioactivity was measured using an automated gamma counter. The distribution coefficient (D) was calculated as [radioactivity (cpm/mL) in *n*-octanol]/[radioactivity (cpm/mL) in phosphate buffer pH 7.4]. The volume was calculated from the mass of the aliquots and the specific density (ρ) of the phase.

2.5. Biodistribution studies

The kinetics and tissue distribution of [^{11}C]SB366791 were studied in normal male Naval Medical Research Institute (NMRI) mice (= control), NMRI mice pretreated (1 h before tracer injection, 10 mg/kg, subcutaneously (s.c.)) with SB366791 or BCTC, a potent and selective TRPV1 antagonist [25], and TRPV1$^{-/-}$ mice. The HPLC-purified tracer was diluted with saline to obtain an ethanol concentration b10%. Mice (body mass 32–43 g) were anaesthetized with pentobarbital (Nembutal, 60 mg/kg intra-peritoneally (i.p.)) or isoflurane (2% in oxygen) and injected with [^{11}C]SB366791 (~9.25 MBq) via a lateral tail vein. The mice were sacrificed by decapitation at 2, 10 or 60 min post injection (p.i., n=4 per time point), dissected and blood, organs and other body parts were collected in tared tubes. The radioactivity in each tube was measured using an automated gamma counter and the tubes containing selected organs and blood were weighed. For calculation of total blood radioactivity, blood mass was assumed to be 7% of the body mass [26].

2.6. Radiometabolites

2.6.1. Plasma radiometabolites—Radiometabolites of [^{11}C]SB366791 in plasma of mice were quantified at 2 and 10 min p.i. of the tracer (n=2 per time point). Mice were anaesthetized with pentobarbital (60 mg/kg; i.p.) and injected with [^{11}C]SB366791 (~ 9.25 MBq) intravenously (i.v.) via a lateral tail vain. The mice were decapitated at the desired time point, blood was collected into lithium heparin-containing tubes (4.5-mL lithium heparin PST tubes, BD Vacutainer; BD, Franklin Lakes, New Jersey) and stored on ice. After centrifugation (3000 rpm; 10 min) of the blood, plasma was separated and analyzed by RP-HPLC on a Chromolith RP C_{18} column (3 mm×100 mm; Merck) eluted with gradient mixtures of CH_3CN (A) and 0.05 M NH_4OAc pH 5.5 (B) (0–4 min: isocratic 0% A, 0.5 mL/min; 4–9 min: linear gradient 0% A to 90% A, 1 mL/min; 9–12 min: isocratic 90% A, 1 mL/min; 12–15 min: linear gradient 90% A to 0% A, 0.5 mL/min). The non-radioactive reference compound SB366791 was co-injected on the Chromolith column to assess the retention time of the intact parent tracer. After passing through a UV detector coupled in series with a 3-in. NaI(Tl) scintillation detector, connected to a single channel analyzer, the HPLC eluate was collected as 0.5-mL or 1-mL fractions (model 2110 fraction collector, Biorad, Hercules, CA). The radioactivity in each fraction was measured using an automated gamma counter.

2.6.2. Brain radiometabolites—Radiometabolites of [^{11}C]SB366791 in brain of mice were quantified at 2 and 10 min after i.v. injection of the tracer (n=2 per time point). Mice were sacrificed by an overdose of pentobarbital (150 mg/kg; i.p.) at the desired time point. The mice were perfused by injection of saline into the left ventricle until the liver turned pale. Brain was isolated and homogenized in a mixture of CH_3CN and water (4 mL, 1:1 V/V). After centrifugation for 10 min at 3000 rpm the supernatant was collected, diluted with CH_3CN (1 mL) and filtered through a 0.22-μm filter (Millipore, Bedford, USA). The filtrate was spiked with SB366791 and analyzed on an analytical RP C_{18} XTerra column (5μm, 4.6 mm×250 mm; Waters) eluted with a mixture of CH_3CN and 0.05 M NH_4OAc pH 5.5 (60:40 V/V) at a flow rate of 1 mL/ min. UV detection was done at 254 nm. The HPLC eluate was collected as 1-mL fractions and radioactivity in each fraction was measured using an automated gamma counter.

2.7. Cell culture

The selected stable CHO cell line expressing rat or human TRPV1 (Tet-Off system) was cultured in maintaining medium (Ham's F-12 supplemented with 10% fetal bovine serum, 0.025 M HEPES pH 7.5, 250μg/mL Geneticin, and 1 mg/L tetracycline).

For [^{3}H]RTX competition binding experiments, cells were seeded in 75 cm^2 culture flasks in maintaining media and grown to approximately 90% confluency after 48 h. The flasks were then washed with DPBS (without Ca^{2+} or Mg^{2+}) and the medium was replaced with inducing medium (Ham's F12 supplemented with 10% fetal bovine serum and 0.025 M HEPES pH 7.3) for an additional 48 h. The cells were harvested in Trypsin-EDTA and DPBS (no Ca^{2+} or Mg^{2+}) and pelleted by centrifugation at 1000 rpm for 5 min. The pellets were stored at −20 °C until use.

2.8. Radioligand binding

Competition binding studies were performed in the presence of a fixed concentration of [^{3}H]RTX and various concentrations of competing ligands. The binding assay mixtures were handled in borosilicate tubes and contained DPBS (with Ca^{2+} and Mg^{2+}), bovine serum albumin (0.25 mg/mL), [^{3}H]RTX (100 pM), and various concentrations of the ligands for a total volume of 350μL. Non-specific binding was determined in the presence of non-radioactive RTX (100 nM). The tubes were incubated for 60 min in a 37 °C water bath. The mixtures were then cooled on ice for approximately 10 min, after which bovine glycoprotein fraction VI (100μL; 2 mg/mL) was added to reduce nonspecific binding. The ice-cold contents were then transferred to 1.5 mL centrifuge tubes for centrifugation. Membrane-bound RTX was separated from free RTX as well as the glycoprotein-bound RTX by pelleting the membranes in a Beckman (Coulter) Allegra 21R centrifuge for 15 min at 12,000 rpm. Radioactivity in the pellets and in an aliquot of each supernatant was determined by scintillation counting in the presence of Cytoscint E.S. (MP Biomedicals). Equilibrium binding parameters (K_i, B_{max}, and cooperativity) were determined by fitting the Hill equation to the measured values.

2.9. $^{45}Ca^{2+}$ uptake experiments

CHO-rTRPV1 or -hTRPV1 cells were plated in 24-well tissue culture plates with maintaining medium and grown to 50%–70% confluency. The following day, the maintaining medium was aspirated and the cells were washed twice with DPBS (no Ca^{2+} or Mg^{2+}). Inducing medium (without tetracycline) was added and the cells were incubated for an additional 48 h to initiate TRPV1 expression. Experiments were done approximately 48 h after induction.

To measure $^{45}Ca^{2+}$ uptake in the assays of agonism, the inducing medium was aspirated and replaced by assay medium (400 μL) in each well. The assay medium consisted of DMEM supplemented with bovine serum albumin (0.25 mg/mL), $^{45}Ca^{2+}$ (37 kBq/mL), and increasing concentrations of the non-radioactive ligand. The cells were incubated for 5 min in a water bath at 37 °C. For a measure of the uptake by a full agonist, a saturating concentration of capsaicin (300 nM) was used. Background uptake was determined in the absence of either compound or capsaicin.

For the antagonism assays, capsaicin (75 nM) was included along with increasing concentrations of the test compound. The cells were incubated for 5 min in a water bath at 37 °C. Immediately after incubation, the assay medium was aspirated and the cells were washed twice with DPBS (no Ca^{2+} or Mg^{2+}). The cells were then lysed in radioimmunoprecipitation assay buffer (50 mM Tris-Cl pH 7.5, 150 mM NaCl, 1% Triton X-100, 1% SDS, and 1% sodium deoxycholate; 400μL/well) for at least 20 min on a shaker. Aliquots (300 μL) of the cell lysates were counted in a liquid scintillation counter.

Each data point in the dose response curves for agonism and antagonism represents the mean of the values from four individual wells. Data from the dose response curves were analyzed by computer fit to the Hill equation. Reported values are the mean of at least three independent experiments unless otherwise indicated.

3. Results and discussion

3.1. Synthesis and radiolabelling

The precursor for radiolabelling (**4**) was synthesized in four steps, starting from 3-acetamidophenol (Fig. 1A). The phenol moiety of 3-acetamidophenol was protected with a 2-tetrahydropyranyl (THP) group. Next, the amine was released by heating in the presence of a strong base. In the third step, EDCI and HOBt were added to activate the carboxylic acid of 4-chlorocinnamic acid for the formation of a peptide bond with the amine of **2** [24]. Finally, the THP group was removed. The non-radioactive reference compound SB366791 was synthesized in two steps (Fig. 1B). First, 4-chlorocinnamic acid was converted into the corresponding acid chloride by reaction with $SOCl_2$. In the following step an amide bond was formed between **5** and 3-methoxyaniline to yield SB366791.

[^{11}C]SB366791 was synthesized via a nucleophilic substitution reaction between the phenolic precursor **4** and the methylating agent [^{11}C]CH_3I as shown in Fig. 2. The reaction mixture was purified using semi-preparative RP-HPLC to remove unreacted [^{11}C]CH_3I and other side-products. Good radiolabelling yields of 69%±11% (range of isolated amounts of radioactivity 3034–5032 MBq) were obtained, based on [^{11}C]CH_3I starting radioactivity. The identity of the tracer was confirmed by co-elution with the non-radioactive reference compound after co-injection on the analytical RP-HPLC system. [^{11}C]SB366791 was obtained within 45 min with high radiochemical purity (N99%) and high specific activity (390±215 GBq/μmol) at end of synthesis.

3.2. Distribution coefficient and polar surface area (PSA)

The lipophilicity of [^{11}C]SB366791 was determined by partitioning between 1-octanol and 0.025 M phosphate buffer pH 7.4. The determined log D value was 3.5±0.1 and is within the optimal range (2.0–3.5) for blood–brain barrier (BBB) penetration [27]. Yet, compounds with a log D between −1 and 4 have been shown to cross the BBB [28]. The ability of a compound to freely cross cell membranes and the BBB is determined by its lipophilicity, PSA (<90 Å^2) [29], extent of protein binding, molecular weight (<450 Da) [29] and charge at physiologic pH. [^{11}C]SB366791 has a calculated PSA of 38.3 Å^2, a molecular weight of 288 Da and is uncharged at physiological pH. These values suggest that [^{11}C]SB366791 may cross the BBB and cell membranes via passive diffusion.

3.3. Biodistribution studies

Control mice were anaesthetized with pentobarbital (60 mg/ kg i.p.) or isoflurane (2% in oxygen) to determine the effect of these anaesthetics on the biodistribution of [^{11}C]SB366791. General anaesthetics such as isoflurane are known to sensitize TRPV1 through interaction on the capsaicin binding place [30]. The binding, shown as standard uptake value (SUV), of [^{11}C]SB366791 in the trigeminal nerve of control mice anaesthetized with isoflurane was remarkable lower than in the case of pentobarbital anaesthesia (Fig. 3A). These results confirm that isoflurane has an unfavourable effect on the ligand-TRPV1 interaction. Therefore, pentobarbital was used as anaesthetic in all further experiments.

The percentage of injected dose (% ID) and percentage of injected dose per gram tissue (% ID/g) at 2, 10 and 60 min after injection of [^{11}C]SB366791 in the control mice anaesthetized with pentobarbital is shown in Table 1. [^{11}C]SB366791 was efficiently cleared from blood (2 min/60 min ratio=4.3) by the hepatobiliary pathway and, to a lesser extent, via the renal pathway. Total initial brain uptake of [^{11}C] SB366791 was high, with 1.6% ID at 2 min after injection and wash-out from brain was rapid (0.1% ID at 60 min p.i.). Prominent is the retention of [^{11}C]SB366791 in the trigeminal nerve (2.9% ID/g at 60 min p.i.; 2 min/60 min ratio=1.5). This persistent *in vivo* binding of the tracer in the trigeminal nerve was absent in mice pretreated with BCTC or SB366791 and in TRPV1$^{-/-}$ mice (data not shown), which suggests specific binding of [^{11}C]SB366791 to the TRPV1 receptor. By calculating the organ-to-blood activity ratios, the uptake of [^{11}C] SB366791 in different organs and tissues can be evaluated independent from activity present in blood. The trigeminal nerve-to-blood activity ratios at 2, 10 and 60 min after injection of the tracer in normal NMRI mice, pretreated mice and TRPV1$^{-/-}$ mice are shown in Fig. 3B. In normal NMRI mice, the activity ratios of the trigeminal nerve (1.2 at 2 min p.i. and 4.1 at 60 min p.i.), spleen, pancreas, skin and bone increase as a function of time. Pretreatment of the mice with BCTC or SB366791 resulted in a significant decrease of the trigeminal nerve-to-blood activity ratios (BCTC: 1.0 at 60 min p.i.; SB366791: 1.3 at 60 min p.i.), a trend that was also observed in TRPV1$^{-/-}$ mice (0.8 at 60 min p.i.). These results suggest specific binding of [^{11}C]SB366791 to the TRPV1 receptor in the trigeminal nerve. No significant difference was observed for the organ-to-blood activity ratios of the spleen, pancreas, skin and bone between control mice, pretreated mice and TRPV1$^{-/-}$ mice (data not shown). The increase of the organ-to-blood activity ratios as a function of time p.i. in spleen, pancreas, skin and bone of control mice is probably due to non-TRPV1 binding of [^{11}C]SB366791 in these tissues or due to an accumulation of radiometabolites.

3.4. Radiometabolites

The metabolic stability of [^{11}C]SB366791 in plasma and brain of male NMRI mice was studied after i.v. injection of HPLC-purified [^{11}C] SB366791 using RP-HPLC. [^{11}C]SB366791 was rapidly metabolized in plasma *in vivo*. At 2 min after injection of [^{11}C]SB366791, 52.0±3.0% of the recovered radioactivity was in the form of intact tracer and 48.0%±3.0% of radiometabolites were found. The percentage of radiometabolites increased from 48.0% ± 3.0% at 2 min p.i. to 82.4%±1.9% at 10 min p.i. All radiometabolites detected were more polar than the intact tracer. The recovery from the HPLC and Chromolith-column injected radioactivity was 92% (n=4).

In brain, 85.6%±3.7% and 67.2%±0.7% of total recovered radioactivity were present as intact tracer at 2 min and 10 min after tracer injection, respectively. As for the plasma metabolites, all radiometabolites detected were more polar than the parent tracer.

3.5. Radioligand binding and $^{45}Ca^{2+}$ uptake experiments

The binding affinity (K_d) of SB366791 for human and rat TRPV1 was determined using [^{3}H]RTX as radioligand. Binding assays were performed on CHO cells transfected with hTRPV1 or rTRPV1, mouse TRPV1 was not available. The binding affinity of SB366791 was found to be 280±56 nM and 780±140 nM for hTRPV1 and rTRPV1, respectively. The

$^{45}Ca^{2+}$ uptake experiments indicated an antagonist activity (K_i) for SB366791 of 197±17 nM against hTRPV1 and 334± 17 nM against rTRPV1. No agonist effects were observed. These data show that SB366791 has a lower affinity for TRPV1 than previously reported with electrophysiological measurements [24]. It is worth mentioning that published affinity and activity data of various TRPV1 ligands show great differences depending on the method as well as within the same type of assay, indicating that these results should be interpreted with care [24,31–33].

Furthermore, SB366791 shows significant species differences in binding affinity and antagonist activity. Species- and modality-specific behavior has previously been observed for capsazepine, another specific TRPV1 antagonist [34]. The retention of [^{11}C]SB366791 in the trigeminal nerve of control mice may be due to species differences, indicating that SB366791 may have a higher binding affinity for mouse TRPV1 compared to rat and human TRPV1. On the other hand and despite the fact that TRPV1 expression has been demonstrated in brain, no accumulation of [^{11}C]SB366791 was observed in the cerebrum nor the cerebellum. We assume that the level of TRPV1 expression in a mouse brain, under normal physiological conditions, is too low to result in sufficient retention of [^{11}C]SB366791. A certain level of target density (B_{max}) is required ($B_{max}/K_d>4$) to obtain site-specific accumulation of a radioligand and to ensure good signal-to-noise ratios [35]. In addition, PET-radioligands must show high binding affinities, preferably in the nM to sub-nM range, and selectivity for the target to enable *in vivo* imaging [28]. The rather low binding affinity of SB366791 for human as well as rat TRPV1 makes the use of [^{11}C] SB366791 for *in vivo* imaging of TRPV1 doubtful.

4. Conclusions

[^{11}C]SB366791 was efficiently radiolabelled in good yields, with high radiochemical purity and high specific activity. Preliminary biological evaluation of [^{11}C]SB366791 showed promising results and retention of [^{11}C]SB366791 was observed in the trigeminal nerve of control mice. Yet, its experimentally observed relatively low binding affinity for rat as well as human TRPV1 makes the use of [^{11}C]SB366791 as a potential PET-radioligand less likely. Moreover, the explicit species differences and the low expression level of TRPV1 under normal physiological conditions complicate the biological evaluation of radioligands that target TRPV1. There is a high need for a well validated, TRPV1-overexpressing animal model to study and validate TRPV1 radioligands. In addition, direct evaluation of TRPV1 specific PET-radioligands in species more closely related to human (e.g. monkeys), without preliminary evaluation in rodents, must be considered.

Acknowledgments

We thank Julie Cornelis (Laboratory for Radiopharmacy, KU Leuven) for her skilful help with the animal experiments. This research was funded by a Ph.D. grant of the Institute for the Promotion of Innovation through Science and Technology in Flanders (IWT), in part by in-vivo molecular imaging research (IMIR) and in part by the Intramural Research Program, National Institutes of Health, National Cancer Institute, Centre for Cancer Research (project Z1A BC 005270).

References

[1]. Caterina MJ, Schumacher MA, Tominaga M, Rosen TA, Levine JD, Julius D. The capsaicine receptor: a heat-activated ion channel in the pain pathway. Nature 1997;389:816–24. [PubMed: 9349813]

[2]. Messeguer A, Planells-Cases R, Ferre-Montiel A. Physiology and pharmacology of the vanilloid receptor. Curr Neuropharmacol 2006;4:1–15. [PubMed: 18615132]

[3]. Pedersen SF, Owsianik G, Nilius B. TRP channels: an overview. Cell Calcium 2005;38:233–52. [PubMed: 16098585]

[4]. Nilius B, Voets T. TRP channels: a TR(I)P through a world of multifunctional cation channels. Eur J Physiol 2005;451:1–10.

[5]. Conway SJ. TRPing the switch on pain: an introduction to the chemistry and biology of capsaicin and TRPV1. Chem Soc Rev 2008;37:1530–45. [PubMed: 18648679]

[6]. Mezey E, Tóth ZE, Cortright DN, Arzubi MK, Krause JE, Elde R, et al. Distribution of mRNA for vanilloid receptor subtype 1 (VR1), and VR1-like immunoreactivity, in the central nervous system of the rat and human. Proc Natl Acad Sci USA 2000;97: 3655–60. [PubMed: 10725386]

[7]. Planells-Cases R, Garcìa-Sanz N, Morenilla-Palao C, Ferrer-Montiel A. Functional aspects and mechanisms of TRPV1 involvement in neurogenic inflammation that leads to thermal hyperalgesia. Pflugers Arch 2005;451:151–9. [PubMed: 15909179]

[8]. Szallasi A, Cruz F, Geppetti P. TRPV1: a therapeutic target for novel analgesic drugs? Trends Mol Med 2006;12:545–54. [PubMed: 16996800]

[9]. Starowicz K, Cristino L, Di Marzo V. TRPV1 receptors in the central nervous system: potential for previously unforeseen therapeutic applications. Curr Pharm Des 2008;14:42–54. [PubMed: 18220817]

[10]. Anand P, Bley K. Topical capsaicin for pain management: therapeutic potential and mechanisms of action of the new high-concentration capsaicin 8% patch. Br J Anaesth 2011;107:490–502. [PubMed: 21852280]

[11]. Moran MM, McAlexander MA, Biro T, Szallasi A. Transient receptor potential channels as therapeutic targets. Nat Rev Drug Discov 2011;10:601–20. [PubMed: 21804597]

[12]. Bodó E, Kovács I, Telek A, Varga A, Paus R, Kovács L, et al. Vanilloid receptor-1 (VR1) is widely expressed on various epithelial and mesenchymal cell types of human skin. J Invest Dermatol 2004;123:410–3. [PubMed: 15245445]

[13]. Charrua A, Reguenga C, Cordeiro JM, Correiade-Sá P, Paule C, Nagy I, et al. Functional transient receptor potential vanilloid 1 is expressed in human urothelial cells. J Urol 2009;182:2944–50. [PubMed: 19846148]

[14]. Akiba Y, Kato S, Katsube K, Nakamura M, Takeuchi K, Ishii H, et al. Transient receptor potential vanilloid subfamily 1 expressed in pancreatic islet β cells modulates insulin secretion in rats. Biochem Biophys Res Commun 2004;321: 219–25. [PubMed: 15358238]

[15]. Szabo T, Biro T, Gonzalez AF, Palkovits M, Blumberg PM. Pharmacological characterization of vanilloid receptor located in the brain. Mol Brain Res 2002;98:51–7. [PubMed: 11834295]

[16]. Roberts JC, Davis JB, Benham CD. [^{3}H]Resiniferatocin autoradiography in the CNS of wild-type and TRPV1 null mice defines TRPV1 (VR-1) protein distribution. Brain Res 2004;995:176–83. [PubMed: 14672807]

[17]. Tóth A, Boczán J, Kedei N, Lizanecz E, Bagi Z, Papp Z, et al. Expression and distribution of vanilloid receptor 1 (TRPV1) in the adult rat brain. Mol Brain Res 2005;135:162–8. [PubMed: 15857679]

[18]. Cavanaugh DJ, Chesler AT, Jackson AC, Sigal YM, Yamanaka H, Grant R, et al. TRPV1 reporter mice reveal highly restricted brain distribution and functional expression in arteriolar smooth muscle cells. J Neurosci 2011;31:5067–77. [PubMed: 21451044]

[19]. Cristino L, de Petrocellis L, Pryce G, Baker D, Guglielmotti V, Di Marzo V. Immunohistochemical localization of cannabinoid type 1 and vanilloid transient receptor type 1 receptors in the mouse brain. Neuroscience 2006; 139:1405–15. [PubMed: 16603318]

[20]. Kauer JA, Gibson HE. Hot flash: TRPV channels in the brain. Trends Neurosci 2009;32:215–24. [PubMed: 19285736]

[21]. Marsch R, Foeller E, Rammes G, Bunck M, Kössl M, Holsboer F, et al. Reduced anxiety, conditioned fear and hippocampal long-term potentiation in transient receptor potential vanilloid type 1 receptor-deficient mice. J Neurosci 2007;27: 832–9. [PubMed: 17251423]

[22]. Gibson HE, Edwards JG, Page RS, Van Hook MJ, Kauer JA. TRPV1 channels mediate long-term depression at synapses on hippocampal neurons. Neuron 2008;57: 746–59. [PubMed: 18341994]

[23]. Morgese MG, Cassano T, Cuomo V, Giuffrida A. Anti-dyskinetic effects of cannabinoids in a rat model of Parkinson's disease: role of CB1 and TRPV1 receptors. Exp Neurol 2007;208:110–9. [PubMed: 17900568]

[24]. Gunthorpe MJ, Rami HK, Jerman JC, Smart D, Gill CH, Soffin EM, et al. Identification and characterization of SB-366791, a potent and selective vanilloid receptor (VR1/TRPV1) antagonist. Neuropharmacology 2004;46:133–49. [PubMed: 14654105]

[25]. Valenzano KJ, Grant ER, Wu G, Hachicha M, Schmid L, Tafesse L, et al. N-(4-tertiarylbutylphenyl)-4-(3-chloropyridin-2-yl)tetrahydropyrazine-1(2H)-car-box-amide (BCTC), a novel, orally effective vanilloid receptor 1 antagonist with analgesic properties: I. In vitro characterization and pharmacokinetic properties. J Pharmacol Exp Ther 2003;306:377–86. [PubMed: 12721338]

[26]. Fritzberg AR, Whitney WP, Kuni CC, Klingensmith W. Biodistribution and renal excretion of 99mTc-N-N′-bis-(mercaptoacetamido) ethylenediamine. Effect of renal tubular transport inhibitors. Int J Nucl Med Biol 1982;9:79–82. [PubMed: 7045000]

[27]. Pike VW. PET radiotracers: crossing the blood–brain barrier and surviving metabolism. Trends Pharmacol Sci 2009;30:431–40. [PubMed: 19616318]

[28]. Clark DE. Rapid calculation of polar molecular surface area and its application to the prediction of transport phenomena. 2. Prediction of blood–brain barrier penetration. J Pharm Sci 1999;88:815–21. [PubMed: 10430548]

[29]. van de Waterbeemd H, Camenisch G, Folkers G, Chretien JR, Raevsky OA. Estimation of blood–brain barrier crossing of drugs using molecular size and shape, and H-bonding descriptors. J Drug Target 1998;6:151–65. [PubMed: 9886238]

[30]. Cornett PM, Matta JA, Ahern GP. General anesthetics sensitize the capsaicin receptor transient receptor potential V1. Mol Pharmacol 2008;74:1261–8. [PubMed: 18689441]

[31]. Appendino G, Harrison S, De Petrocellis L, Daddario N, Bianchi F, Moriello AS, et al. Halogenation of a capsaicin analogue leads to novel vanilloid TRPV1 receptor antagonists. Br J Pharmacol 2003;139:1417–24. [PubMed: 12922928]

[32]. Gavva NR, Tamir R, Qu Y, Klionsky L, Zhang TJ, Immke D, et al. AMG 9810 [(E)-3-(4-t-butylphenyl)-N-(2,3-dihydrobenzo[b][1,4]dioxin-6-yl)acrylamide], a novel vanilloid receptor 1 (TRPV1) antagonist with antihyperalgesic properties. J Pharmacol Exp Ther 2005;313:474–84. [PubMed: 15615864]

[33]. Varga A, Németh J, Szabó Á, McDougall JJ, Zhang C, Elekes K, et al. Effects of the novel TRPV1 receptor antagonist SB366791 in vitro and in vivo in the rat. Neurosci Lett 2005;385:137–42. [PubMed: 15950380]

[34]. Seabrook GR, Sutton KG, Jarolimek W, Hollingworth GJ, Teague S, Webb J, et al. Functional properties of the high-affinity TRPV1 (VR1) vanilloid receptor antagonist (4-hydroxy-5-iodo-3-methoxyphenylacetate ester) iodo-resiniferatoxin. J Pharmacol Exp Ther 2002;303:1052–60. [PubMed: 12438527]

[35]. Passchier J, Gee A, Willemsen A, Vaalburg W, van Waarde A. Measuring drug-related receptor occupancy with positron emission tomography. Methods 2002;27:278–86. [PubMed: 12183116]

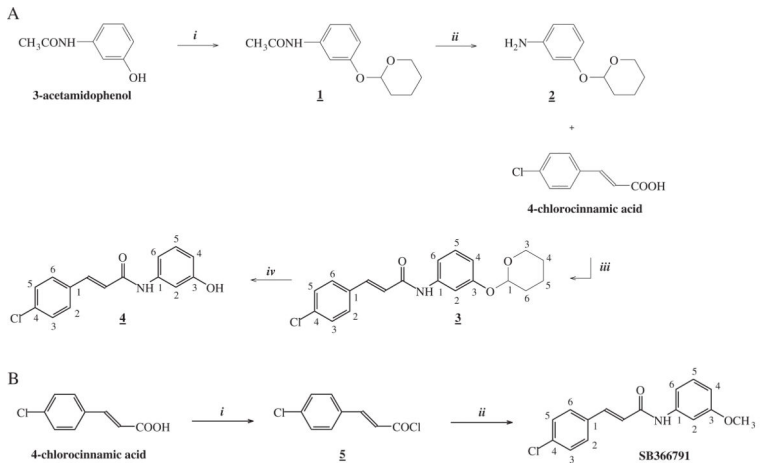

Fig. 1.

A. Synthesis of the precursor *N*-(3-hydroxyphenyl)-4-chlorocinnamide (**4**). **i.** CH_2Cl_2, PPTS, 3,4-dihydro-2 H-pyran under N_2 for 16h. **ii.** NaOH, ethylene glycol at 130 °C for 4 h. **iii.** EDCI, HOBt at room temperature for 16 h. **iv.** PPTS, EtOH at 45 °C for 18 h. **B.** Synthesis of the reference compound SB366791. **i.** $SOCl_2$, reflux for 2 h. **ii.** 3-methoxyaniline, toluene, NEt_3 at room temperature for 2 h.

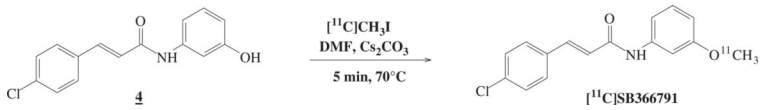

Fig. 2.
Radiolabelling of precursor **4** yielding [^{11}C]SB366791.

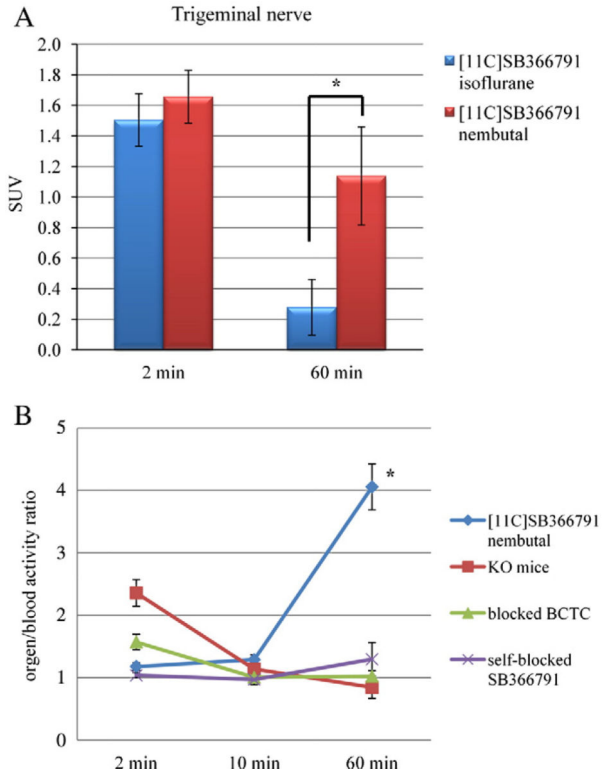

Fig. 3.

A. SUV of [^{11}C]SB366791 in the trigeminal nerve of control mice anaesthetized with isoflurane (2% in oxygen; in blue) or pentobarbital (Nembutal, 60 mg/kg i.p.; in red) at 2 and 60min p.i. of the tracer (n=4 per time point). **B.** Trigeminal nerve-to-blood activity ratios of [^{11}C]SB366791 in control mice, mice pretreated with BCTC or SB366791 (10 mg/kg; 1 h before injection of the tracer; s.c.) and TRPV1$^{-/-}$ mice at 2, 10 and 60 min p.i. of the tracer (n=4 per time point). Data are expressed as mean± standard error of the mean.

Table 1

Tissue distribution of [^{11}C]SB366791 in control mice at 2,10 and 60 min p.i.(n=4 per time point).

[^{11}C]SB366791	**% ID**[a]			**% ID/g**[b]		
	2min	**10min**	**60min**	**2 min**	**10min**	**60min**
Bladder+urine	0.2±0.1	8.0±2.5	25.9±12.0	-	-	-
Kidneys	4.5±0.2	5.0±1.0	1.9±0.4	7.1±0.8	7.9±1.2	2.8±0.5
Liver	28.6±2.5	16.1±1.6	8.9±3.2	14.2±2.5	8.7±1.0	4.6±2.1
Spleen	0.6±0.2	0.2±0.0	0.2±0.0	4.0±0.8	2.0±0.2	1.4±0.3
Pancreas	1.1±0.1	0.6±0.1	0.5±0.2	5.4±0.9	2.7±0.2	2.0±0.5
Lungs	1.5±0.4	0.9±0.2	0.5±0.2	4.5±0.3	2.7±0.1	1.6±1.0
Heart	0.9±0.1	0.3±0.1	0.1±0.0	5.0±1.0	1.8±0.2	0.6±0.0
Intestines	8.9±0.6	13.0±1.5	33.8±6.2	-	-	-
Stomach	1.4±0.2	2.0±0.7	1.8±0.7	-	-	-
Cerebrum	1.2±0.2	0.4±0.0	0.1±0.0	3.7±0.5	1.2±0.1	0.3±0.0
Cerebellum	0.4±0.1	0.1±0.0	0.0±0.0	3.9±0.4	1.1±0.1	0.3±0.1
Blood	9.9±1.0	6.9±0.5	2.3±0.2	3.6±0.4	2.6±0.2	0.8±0.1
Bone	-	-	-	1.5±0.2	1.2±0.4	0.9±0.2
Muscle	-	-	-	1.2±0.3	1.3±0.2	0.4±0.1
Skin	-	-	-	1.3±0.1	2.4±0.3	1.1±0.3
Trigeminal nerve	0.02±0.00	0.01±0.00	0.01±0.00	4.2±0.4	3.4±0.2	2.9±0.7
Carcass	44.5±3.6	48.6±2.2	19.3±3.3	-	-	-

Mice were anaesthetized with pentobarbital (60 mg/kg i.p.) and injected i.v. with ~9.25 MBq. Data are expressed as mean±standard deviation.

[a]Percentage of injected dose calculated as counts per minute in organ/total counts per minute recovered.

[b]Percentage of injected dose per gram tissue.